

# VLT-ISAAC 3–5 $\mu\text{m}$ spectroscopy of low-mass young stellar objects: prospects for CRIREs

Klaus M. Pontoppidan<sup>1</sup> and Ewine F. van Dishoeck<sup>1</sup>

Leiden Observatory, P.O. Box 9513, NL-2300 RA Leiden, Netherlands

**Abstract.** We present results from an extensive spectroscopic survey in the 3–5  $\mu\text{m}$  wavelength region of low-mass young stellar objects using VLT-ISAAC. Medium resolution spectra ( $\lambda/\Delta\lambda \sim 1000 - 10000$ ) of young embedded stars in the mid-infrared allow for detailed studies of ro-vibrational lines from molecular gas, interstellar ices and Polycyclic Aromatic Hydrocarbons (PAHs). By taking advantage of this wide range of molecular tracers available within a few spectral settings, the survey has helped to constrain the chemical evolution of cold molecular material in low-mass star forming regions as well as the physics of disks surrounding protostars. In this contribution, we will review the various spectral diagnostics of molecular material, which require ground-based high resolution infrared spectroscopy. The importance of a high resolution spectroscopic capability as will be offered by CRIREs is discussed in the context of the physics and chemistry of low-mass star formation.

## 1 Introduction

The earliest stages of star- and planet formation are characterised by enormous amounts of gas and dust (up to several hundred mag of extinction) on scales of a few thousand AU. Since the young star itself is often invisible, spectroscopic observations of the surrounding material are the only way to probe the physical and chemical processes that take place deep inside the circumstellar envelope. High resolution infrared spectroscopy is a particularly powerful tool to study these early phases, and gives information that is quite complementary to that obtained from submillimeter emission lines.

The atmospheric windows from 3–5  $\mu\text{m}$  contain a range of important spectroscopic tracers of circumstellar material. These include vibrational bands of solid-state volatiles, such as water ice at 2.8–3.8  $\mu\text{m}$ ,  $^{12}\text{CO}$  ice at 4.67  $\mu\text{m}$  and  $^{13}\text{CO}$  ice at 4.78  $\mu\text{m}$  in addition to weaker bands from solid  $\text{CH}_3\text{OH}$ ,  $\text{H}_2\text{CO}$ ,  $\text{OCN}^-$ ,  $\text{OCS}$ . Also the C-H stretching band from Polycyclic Aromatic Hydrocarbons (PAHs) at 3.3  $\mu\text{m}$  is easily observable. A vast number of ro-vibrational lines from gas-phase molecules are in principle present throughout the mid-infrared wavelength range. The bands most easily accessible from the ground are the CO overtone bandheads around 2.3  $\mu\text{m}$  and the CO fundamental band around 4.67  $\mu\text{m}$ , but also water vapour,  $\text{CH}_4$  and possibly  $\text{CH}_3\text{OH}$  gas can be observed from the ground, albeit with considerable difficulty [6][12].

While ground-based mid-infrared spectroscopic observations are limited in sensitivity and wavelength coverage by atmospheric emission and absorption, respectively, they outperform current space-based spectroscopy by orders of magnitudes in terms of spatial and spectral resolution. For example, the recently

launched Spitzer Space Telescope can produce good quality spectra with signal-to-noise ratios sufficient for ice absorption line studies of sources fainter than 10 mJy in the 5–20  $\mu\text{m}$  wavelength region. However, this is with a spectral resolving power of only  $\lambda/\Delta\lambda \sim 100 - 600$  and a spatial resolution of 2–6", depending on wavelength. For comparison, VLT-ISAAC reaches an effective signal-to-noise ratio of  $\sim 10 - 20$  at 4.7  $\mu\text{m}$  for a 100 mJy source, but with a spectral resolution of  $\lambda/\Delta\lambda \sim 10\,000$  and a typical spatial resolution of 0.2–0.4". VISIR offers similar capabilities in the *N*- and *Q*-bands and CRIRES will add another order of magnitude to the spectral resolution in the 3–5  $\mu\text{m}$  region. As will be discussed below, such high spectral resolution is essential to reliably measure the intrinsically very narrow gas-phase lines as well as observe narrow substructure in solid-state features.

In this contribution, we present results from 5 years of dedicated *L*- and *M*-band spectroscopic observations with ISAAC of interstellar gas and dust in low-mass star-forming regions. Finally, we will discuss observational strategies for the future.

## 2 Summary of observations and importance of high spectral resolution

A total of 60 lines of sight in the Ophiuchus, Chamaeleon, Corona Australis, Vela, Orion and Serpens star-forming regions have been observed in the 2.8–4.2  $\mu\text{m}$  and 4.55–4.8  $\mu\text{m}$  regions and 15 lines of sight have been observed in one wavelength region only. Of these, 80% show the presence of ice while 70% show ro-vibrational lines from CO. Good quality spectra with signal-to-noise ratios in excess of 15 were obtained of sources as faint as 20 mJy at 3.5  $\mu\text{m}$  and 100 mJy at 4.7  $\mu\text{m}$ . All of the ice features are seen in absorption against the hot ( $T_{\text{dust}} > 300$  K) dust in the immediate surroundings of the young star, whereas the gas-phase lines are seen both in absorption and emission.

In general, the 2.8–4.2  $\mu\text{m}$  region was observed using the ISAAC low resolution module giving resolving powers of  $R = \lambda/\Delta\lambda = 600 - 1200$ , depending on the slit width. This is sufficient for getting high quality spectra of the broad 3  $\mu\text{m}$  water ice band. However, there are instances where higher spectral resolution significantly improves the quality of solid state spectra, especially in wavelength regions dominated by complex telluric absorption. Telluric absorption lines are intrinsically narrow ( $\sim 5 \text{ km s}^{-1}$ ) and therefore always unresolved with the present instrumentation. By going to higher spectral resolution, it becomes easier to identify the sections of the spectrum where spectral information is lost or heavily affected due to strong or saturated telluric lines. For the interpretation of shallow substructure in ice bands, this becomes increasingly relevant. For instance, in order to properly confirm detections of the weak 3.53  $\mu\text{m}$  band from solid methanol ( $\text{CH}_3\text{OH}$ ), a spectrum using the high resolution module was often taken to improve the telluric correction at  $R=3000 - 6000$ . Another example is the 3.3  $\mu\text{m}$  PAH feature which is often difficult to separate from the 3.30  $\mu\text{m}$  Pf  $\delta$  hydrogen recombination line in the low resolution module.

In the  $M$ -band at 4.5–5.0  $\mu\text{m}$ , we found that the highest resolution available with ISAAC of  $R=10\,000$  gave the best result. This was partly due to the presence of many ro-vibrational lines from gaseous CO and partly due to the presence of narrow substructure in the 4.67  $\mu\text{m}$  CO ice band. The circumstellar CO gas phase lines are known in some cases to be as narrow as a few  $\text{km s}^{-1}$ , i.e. much less than the best resolution of ISAAC of  $30\text{ km s}^{-1}$ . Traditionally, telluric lines are removed by dividing with a spectrum of an intrinsically featureless standard star. However, this procedure assumes that the convolution with an instrument profile of a product of two spectra is the product of each spectrum convolved with the instrument profile. This is clearly only valid when the instrument profile is negligible, i.e. when the features in the spectrum are completely resolved or when the telluric spectrum is approximately constant.

There are two realistic solutions to this fundamental problem. The first is to go to higher resolving power which will be offered by CRIRES, and the second is to observe the spectrum at a time of the year when the line of interest is shifted away from the telluric features. The first option is the better, since even reasonably small variations in the telluric spectrum can shift and distort astronomical lines. Fig. 1 shows an example of the effect of telluric lines on an unresolved CO ro-vibrational line. For a Doppler shift of  $10\text{ km s}^{-1}$ , the derived line strength can be more than a factor of 2 wrong at the best resolution of ISAAC, while a Doppler shift of  $20\text{ km s}^{-1}$  causes smaller, but non-negligible errors. Clearly, for this type of line, a spectral resolving power of more than 50 000 is required to obtain robust line strengths, centers and profiles. For our ISAAC sample, the problem is most clearly illustrated by the almost total absence of any CO ro-vibrational lines toward sources in the Chamaeleon star-forming cloud, where the shift at a declination of  $-77^\circ$  is always less than  $10\text{ km s}^{-1}$  for nearby molec-

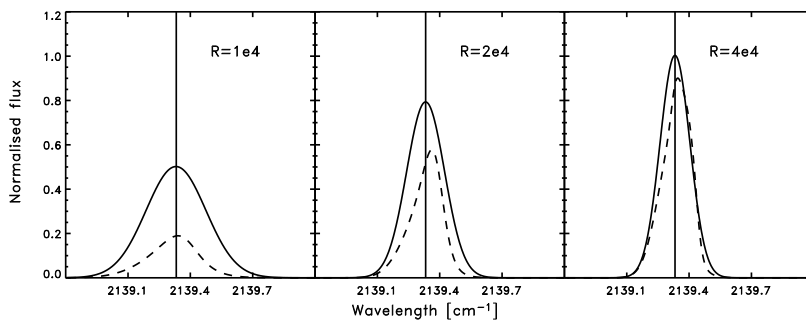


**Fig. 1.** A simulation of the effect on the recovered profile of an unresolved line by simple division with a telluric standard star. The full line shows the intrinsic line profile as it should appear when observed at the relevant resolution. The dashed line shows the profile obtained after standard correction for the telluric absorption spectrum. The specific case shown is for the  $^{12}\text{CO P}(1) \nu=1-0$  line at  $2139.43\text{ cm}^{-1}$  for a line width of  $15\text{ km s}^{-1}$  and a Doppler shift of  $10\text{ km s}^{-1}$ . A telluric spectrum observed at a resolving power of  $\lambda/\Delta\lambda = 100\,000$  was used for the calculation.

ular clouds. Thus, this should not be interpreted as a real lack of lines. To ensure that the effect of telluric lines is small, the velocity shift should be at least one resolution element, or the astronomical lines should be resolved.

### 3 General results

#### 3.1 Overview

An overview of our results, together with illustrative spectra, is presented in [19]. Some of the highlights include the first detection of solid methanol in low-mass protostars, a key ingredient for building more complex organic molecules [15]; direct evidence for significant freeze-out in edge-on circumstellar disks [18]; sensitive limits on minor ice components such as ammonia and deuterated water [7,17,8]; and a new weak feature at  $2175\text{ cm}^{-1}$  ( $4.61\text{ }\mu\text{m}$ ) which may be due to CO directly bound to the silicate surface [9].

The unprecedented combination of high spectral resolution and high  $S/N$  has also allowed the solid CO band at  $4.67\text{ }\mu\text{m}$  to be fully resolved and to be studied for a large number of sources [14]. Surprisingly, excellent fits to *all* our spectra can be obtained using a phenomenological decomposition into just three components, with only the relative strength of these components changing from object to object. This leads to the important conclusion that the CO ice has the same fundamental structure along all lines of sight. For most sources, a significant fraction of the CO is in nearly pure form, i.e., not mixed with H<sub>2</sub>O ice. This presents a puzzle to theories of ice mantle formation: either the segregation of the CO and other species has occurred prior or during freeze-out, or subsequent processing of the ice and selective desorption and recondensation have resulted in separation of the components.

In some sources, the <sup>12</sup>CO ice feature is so strong that its isotopic <sup>13</sup>CO counterpart has been detected. Since <sup>13</sup>CO is only a minor component of the ice, its line shape does not depend on the grain shape and allows further constraints to be placed on the CO ice environment. Because the <sup>13</sup>CO ice band is not broadened by grain shape effects, it becomes extremely narrow and requires resolving powers in excess of  $R = 10\,000$  in order to be fully resolved. In addition, the band is often blended with ro-vibrational CO gas-phase lines, and a high spectral resolution is essential to disentangle the two phases. In Fig. 2 is shown an example of a <sup>13</sup>CO ice band.

#### 3.2 Peculiar sources

While most  $3\text{--}5\text{ }\mu\text{m}$  spectra of low-mass young stellar objects have similar characteristics, a few peculiar objects were identified. Here, two examples are described.

*IRS 48 (WLY 2-48)* Almost none of the observed low-mass YSOs show compact emission in the  $3.3\text{ }\mu\text{m}$  band of polycyclic aromatic hydrocarbons (PAHs). While extended emission from PAHs is seen throughout molecular clouds and compact

emission is seen from disks around some Herbig Ae stars, clear PAH features are rarely seen toward low-mass YSOs. However, IRS 48 ( $L = 7.4 L_{\odot}$ ) in the  $\rho$  Oph cloud has a very strong and compact ( $<80$  AU)  $3.3 \mu\text{m}$  PAH band with a peak flux over the continuum of almost 1 Jy. The  $L$ -band spectrum of IRS 48 is shown in Fig. 3. IRS 48 is classified as a low-mass flat spectrum YSO [4]. It is an interesting question whether the compact PAH emission from embedded protostars is due to a circumstellar disk as that of the more evolved Herbig Ae stars [3][10].

*GSS 30 IRS 1* This embedded star in the Ophiuchus cloud core exhibits the highest ro-vibrational CO line-to-continuum ratio of our sample. The lines are spatially extended to a distance of  $2'' = 320$  AU from the central source. These two properties make this source unique among the observed CO emission line sources. Radiative transfer modeling has shown that the lines can be reproduced by a single temperature gas of a little over 500 K. However, to simultaneously model the optical depth, the high line flux level and the observed spatial extent of the line emission, it was found that lines emitted from the central 20 AU of a circumstellar disk must be scattered in the bipolar cavity also seen in near-infrared imaging. The single temperature can then be explained as a cooling plateau behind a shock, possibly an accretion shock, on the surface of an embedded circumstellar disk. The peculiar geometry of the source thus enabled a study of the physics of a region normally obscured from view by a dense and dusty envelope. However, the lines were not spectrally resolved by ISAAC and only barely resolved at  $R=25\,000$  in subsequent Keck spectroscopy. Thus, this

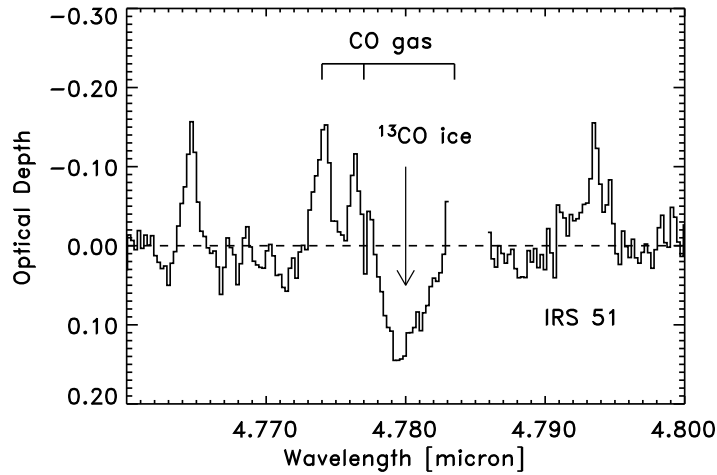


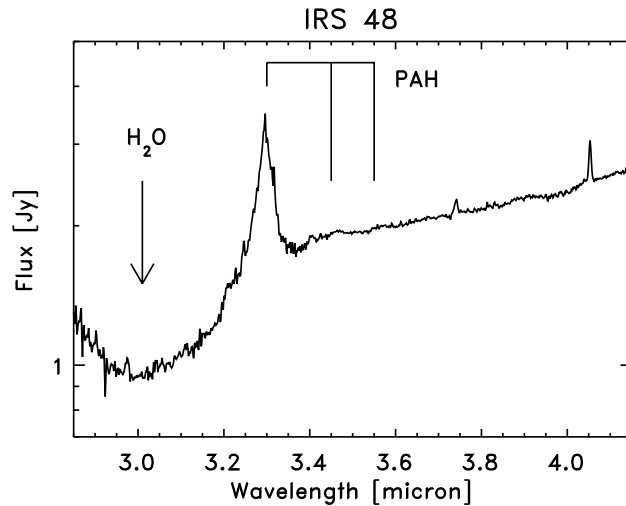
**Fig. 2.** The  $^{13}\text{CO}$  ice band observed toward IRS 51 in Ophiuchus, from [14].

is clearly a case where ground-based high resolution spectroscopy is required to learn more.

#### 4 CO ro-vibrational lines from embedded young low-mass stars

The CO ro-vibrational lines observed toward embedded stars show very diverse structures, ranging from very deep absorption lines to bright emission lines. Also, the line widths vary from unresolved at  $\lambda/\Delta\lambda = 10\,000$  or  $20\text{ km s}^{-1}$  to being as wide as  $100\text{ km s}^{-1}$ . Some sources show different velocity components with widely different optical depths and excitation temperatures in absorption along the line of sight. Disentangling all the gas components that contribute to the CO ro-vibrational spectra in many sources clearly requires higher spectral resolution spectroscopy with CRIRES.

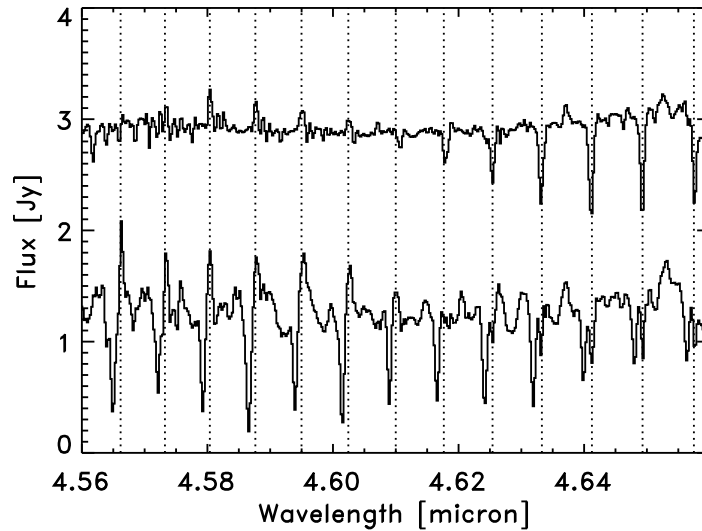
An interesting example of a complex ro-vibrational CO case is presented in Figure 4, which shows separate  $4.6\text{ }\mu\text{m}$  spectra of each component of the low-mass binary YSO EC 90 in the Serpens core. The two components are separated by only  $1.6'' = 400\text{ AU}$ , yet the line spectra differ dramatically. Both lines of sight show similar contributions from cool gas near zero velocity while EC 90B shows an additional warm, narrow component shifted by  $80\text{ km s}^{-1}$ . Finally, broad emission lines are seen from EC 90B near zero velocity. It is tempting to conclude that the cool component seen toward both components is due to a circumbinary envelope, while the complex line structure toward EC 90B is due to activity in the inner disk of this star, possibly related to an outflow along the line of sight.



**Fig. 3.** *L*-band spectrum of IRS 48 showing bright PAH  $3.3\text{ }\mu\text{m}$  emission and a shallow  $3.01\text{ }\mu\text{m}$  water ice band in absorption.

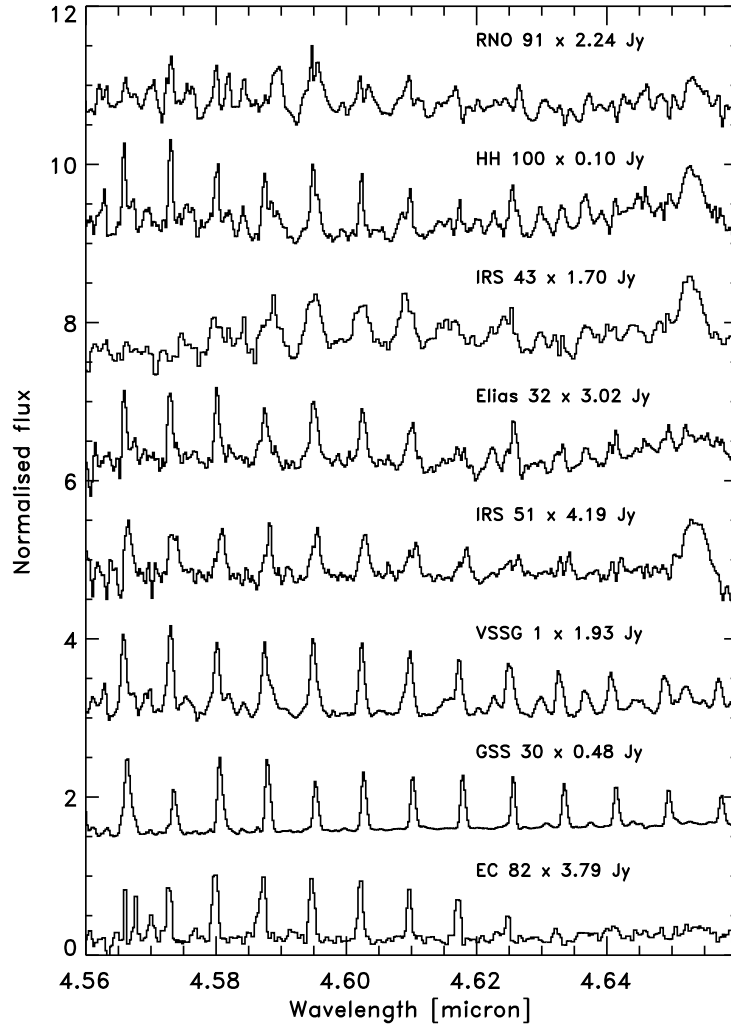
It is not clear, however, how a compact clump of gas is accelerated to a narrow range of velocities around  $80 \text{ km s}^{-1}$  as evidenced by the strongly shifted, yet unresolved lines. Such extremely high velocity clumps or ‘bullets’ have been detected previously only at millimeter wavelengths in even more deeply embedded Class 0 objects, e.g. [1].

Figure 5 shows a gallery of ro-vibrational emission lines toward embedded objects. The gallery is ordered according to increasing complexity of the line spectrum, such that spectra showing broad lines with bright  $^{13}\text{CO}$  lines and  $^{12}\text{CO } \nu=2-1$  lines are at the top and spectra dominated by narrow  $^{12}\text{CO } \nu=1-0$  lines at the bottom. [2] recently published a survey of CO ro-vibrational emission lines from Herbig Ae stars, i.e., somewhat older and more massive objects than those presented here. They find that a significant part of the line emission must be excited by resonance fluorescence and that the line widths correlate well with disk inclination. An interesting question is whether the emission lines observed toward embedded objects exhibit the same characteristics. The least complex spectra with narrow lines and weak  $^{13}\text{CO}$  lines and  $^{12}\text{CO } \nu=2-1$  lines resemble the older Herbig Ae disks the most. However, some of the spectra of embedded sources show  $^{13}\text{CO}$  lines and  $^{12}\text{CO } \nu=2-1$  lines which are almost as bright as the  $^{12}\text{CO}$  fundamental lines. This indicates both high optical depths as well as high excitation temperatures in excess of 700 K. In addition, the de-reddened luminosity in the ro-vibrational CO band is in some cases 1-2 orders of



**Fig. 4.** Comparison of the CO ro-vibrational lines from each component of the  $1.6''$  binary YSO EC 90 in the Serpens core. The dotted lines indicate the positions of the ro-vibrational transitions of  $^{12}\text{CO}$  to the first vibrationally excited level.

magnitudes higher in embedded sources compared to the Herbig Ae disks of [2], although the intrinsic scatter is large. This suggests that a different mechanism may produce the ro-vibrational emission in embedded stars. One possibility is cooling emission excited by accretion activity as proposed by [13].



**Fig. 5.** Gallery of CO ro-vibrational emission lines observed toward embedded low-mass YSOs ordered according to complexity. The spectra have been scaled by the amount indicated in the figure and shifted for clarity. Broad absorption bands from ices have been removed from the spectra of RNO 91, HH 100, IRS 43, Elias 32 and IRS 51.



## 5 Mapping ices on 1000 AU scales in a protostellar envelope

A new possibility in mid-infrared spectroscopy is the spatial mapping of ice abundances in protostellar regions [16]. This has been facilitated mainly by the increase in sensitivity of both ground- and space-based infrared spectrometers rather than by developments in spectral resolution. However, high resolution spectroscopy in principle allows for a simultaneous determination of the ice-to-gas ratio along a specific line of sight for the chemical species observed; the ice column density can be obtained from a stretching mode ice band, while the gas column density can be determined from absorption in the associated ro-vibrational band. This has been taken advantage of in the past for isolated lines of sight, e.g. [5][18]. In order to unambiguously determine gas column densities from ro-vibrational absorption lines, it is necessary to spectrally resolve the lines. Since lines from cold molecular gas will have widths of less than  $5 \text{ km s}^{-1}$ , spectroscopy at  $R = 100\,000$  is in principle necessary.

Fig. 6 shows the water ice abundance as a function of distance to the center of the class 0 protostar SMM 4 in the Serpens cloud core. The abundances were determined using observations of the  $3.01 \mu\text{m}$  water ice band toward sources located in a small stellar cluster embedded in the envelope of SMM 4. The observed sources are spaced only 1000–2000 AU apart, and the resulting water ice map thus has a spatial resolution two orders of magnitude better than any previous maps. The abundance of water ice remains constant throughout most of the envelope, but the point closest to the center of SMM 4 shows an increase in abundance by a factor of 1.7. This is consistent with recent models predicting a jump in gas phase depletion at the density where the freeze-out timescale becomes smaller than the collapse timescale [11]. Similar observations of the  $3.53 \mu\text{m}$  methanol ice band shows that the abundance of methanol ice is enhanced by a factor of 10 to an abundance of  $3 \times 10^{-5}$  with respect to  $\text{H}_2$  relative to the surrounding cloud medium in Serpens. The cause of this enhancement of the methanol ice abundance is presently not known.

## 6 Acknowledgments

The VLT-ISAAC survey was carried out in close collaboration with E. Dartois, W.F. Thi, L. d’Hendecourt, A. Boogert, H. Fraser, S. Bisschop, W. Schutte and A. Tielens. Research in Astrochemistry in Leiden is supported by grants from the National Research School for Astronomy (NOVA) and a Spinoza grant from NWO.

## References

1. Bachiller, R., Martín-Pintado, J., and Planesas, P., *A&A*, 251, 639 (1991)
2. Blake, G. A. and Boogert, A. C. A., *ApJ*, 606, L73 (2004)

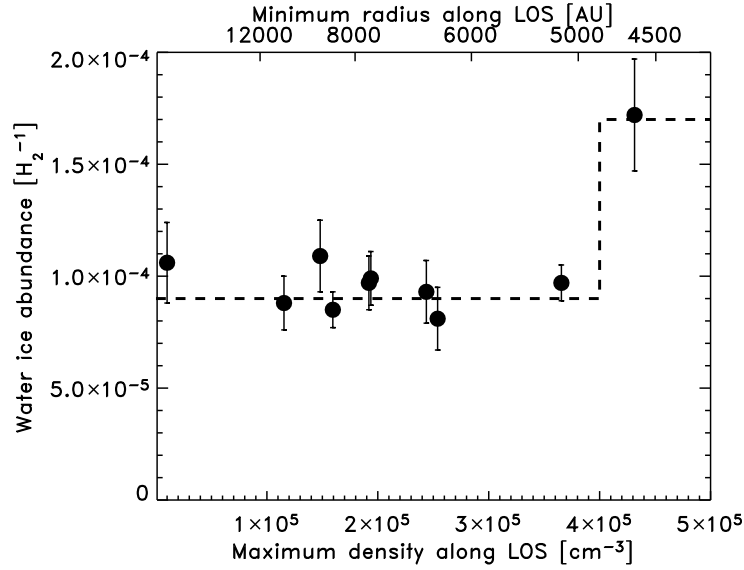


**Fig. 6.** The abundance of water ice with respect to  $\text{H}_2$  in the envelope of the class 0 protostar SMM 4 in the Serpens cloud core as a function of distance to the envelope center. The dashed line indicates the location of an apparent jump in the abundance of water ice.

3. van Boekel, R., Waters, L. B. F. M., Dominik, C., Dullemond, C. P., Tielens, A. G. G. M., & de Koter, A, *A&A*, 418, 177 (2004)
4. Bontemps, S., et al., *A&A*, 372, 173 (2001)
5. Boonman, A. M. S. & van Dishoeck, E. F., *A&A*, 403, 1003 (2003)
6. Carr, J. S., Tokunaga, A. T., and Najita, J., *ApJ*, 603, 213 (2004)
7. Dartois, E., d'Hendecourt, L., Thi, W.-F., Pontoppidan, K. M. and van Dishoeck, E. F., *A&A* 394, 1057 (2002)
8. Dartois, E., Thi, W.-F., Geballe, T. R., Deboffle, D., d'Hendecourt, L. and van Dishoeck, E. F., *A&A* 399, 1099 (2003)
9. Fraser, H. J. et al., in prep (2004)
10. Geers, V. C. et al., this volume (2004)
11. Jørgensen, J. K., Schöier, F. L., & van Dishoeck, E. F., *A&A*, 416, 603 (2004)
12. Lacy, J. H., Carr, J. S., Evans, N. J., Baas, F., Achtermann, J. M. and Arens, J. F., *ApJ*, 376, 556 (1991)
13. Pontoppidan, K. M., Schöier, F. L., van Dishoeck, E. F. and Dartois, E., *A&A*, 393, 585 (2002)
14. Pontoppidan, K. M., Fraser, H. J., Dartois, E., Thi, W.-F., van Dishoeck, E. F., Boogert, A. C. A., d'Hendecourt, L., Tielens, A. G. G. M. and Bisschop, S. E., *A&A*, 408, 981 (2003)
15. Pontoppidan, K. M., Dartois, E., van Dishoeck, E. F., Thi, W.-F. and d'Hendecourt, L., *A&A*, 404, L17 (2003)

16. Pontoppidan, K. M., van Dishoeck, E. F. and Dartois, E., *A&A*, submitted (2004)
17. Taban, I. M., Schutte, W. A., Pontoppidan, K. M., and van Dishoeck, E.F., *A&A*, 399, 169 (2003)
18. Thi, W.-F., Pontoppidan, K. M., van Dishoeck, E. F., Dartois, E. and d'Hendecourt, L., *A&A* 394, L27 (2002)
19. van Dishoeck, E.F., Dartois, E., Pontoppidan, K.M., et al., *Messenger*, 113, 49 (2003)